Journal of Hydroscience and Hydraulic Engineering
Vol. 2, No. 2, November, 1984. pp.35-44.

NEAR FIELD BEHAVIOR OF THREE-DIMENSIONAL BUOYANT SURFACE DISCHARGES

By

Akira Murota
Professor, Department of Civil Engineering

Keiji Nakatsuji
Assistant Professor, Department of Civil Engineering

and

Yuichi Shibagaki
Post-Graduate Student

Osaka University, Suita City, Osaka 565, Japan

SYNOPSIS

The near field behavior of three-dimensional buoyant surface discharges has been investigated theoretically based on the basic conservation equations in terms of an integral formulation of mass flux, buoyancy flux and momentum flux in the streamwise direction. It shows that the near field behavior can be classified into four flow regimes depending on a newly-defined parameter, $Sd = E_V(2B/H)/(dB/dx)$ in addition to the densimetric Froude number, Fd. The result suggests that the lateral spread of discharged buoyant water is intimately related with not only the vertical entrainment rate but also its aspect ratio. Furthermore, it has been demonstrated that the proposed integral formulation can predict a flow acceleration of river effluent expansion and a three-dimensional spread of thermal discharge very well.

INTRODUCTION

The basic physical processes important to the dispersion of momentum and buoyancy within buoyant surface discharges are : jet entrainment, buoyant spreading, crossflow interaction, diffusion induced by ambient-turbulence and surface heat exchange. The last three processes are related with environmental circumstances. In the regions of great interest, the near and intermediate fields, the other two are of significant importance in modeling. In particular, as the buoyancy promotes the gravitational stability very much, the vertical entrainment tends to reduce even near an outfall, and a discharged water body spreads above the sea surface. This tendency is evidently observed in river effluents, which spread on all sides just like a potential flow before long from a river mouth.

The field surveys and observations(1) indicate that the internal interface of river effluent is so fairly stable that even great disturbances such as wind waves of 1 m wave-height can not raise the vertical mixing across its interface. The similar results(2) were obtained experimentally that the lateral entrained volume is larger than the vertical one in a buoyant surface jet. As above-mentioned, the buoyancy has direct effects on the near field behavior of buoyant surface discharges in two functions : (1) reduction of the vertical entrainment and (2) lateral gravitational spread. As both functions are closely correlated, it is necessary to introduce them skillfully in modeling so as not to be contradictory each other.

The present study is to make clear a relationship between the vertical entrainment rate and the lateral spread in connection with discharged flow

behavior through an integral formulation of basic conservation equations, and to demonstrate numerical results such as river effluent expansion and thermal discharges. A part of this paper has already been reported by the authors in Japanese paper(3).

GOVERNING EQUATIONS

For a Cartesian system with coordinates x, y and z as sketched in Fig.1, the steady equations describing the water flow discharged with buoyancy incorporating the Boussinesq approximation and the boundary layer one, are :

$$\frac{\partial U}{\partial x} + \frac{\partial V}{\partial y} + \frac{\partial W}{\partial z} = 0 \tag{1}$$

$$\frac{\partial}{\partial x}(U\Delta\rho) + \frac{\partial}{\partial y}(V\Delta\rho) + \frac{\partial}{\partial z}(W\Delta\rho) = \frac{\partial}{\partial y}(-\overline{\rho v}) + \frac{\partial}{\partial z}(-\overline{\rho w}) \tag{2}$$

$$\frac{\partial}{\partial x}(\rho U^2) + \frac{\partial}{\partial y}(\rho UV) + \frac{\partial}{\partial z}(\rho UW) = -\frac{\partial P}{\partial x} + \frac{\partial}{\partial y}(-\overline{\rho uv}) + \frac{\partial}{\partial z}(-\overline{\rho uw}) \tag{3}$$

$$\frac{\partial P}{\partial z} = \rho g - \rho_a \frac{\partial}{\partial z}(\overline{w^2}) \tag{4}$$

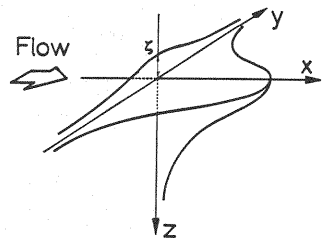

Fig. 1 Sketch of flow field

For these equations, U, V, W = velocity components in x, y, z directions, u, v, w = fluctuating parts of velocity components, ρ = density, $\Delta\rho = \rho - \rho_a$, ρ_a = density of ambient water, P = pressure, g = gravitational acceleration, $-\overline{\rho v}$, $-\overline{\rho w}$ = turbulent density flux, $-\overline{uv}$, $-\overline{uw}$ = turbulent momentum flux, and overscore '-' = time mean.

The mean pressure is approximately given by means of integration of Eq. 4 over the range of $z = -\zeta$ and $z = z$.

$$P(x,y,z) = \int_{\zeta}^{z} \rho g \, dz - \rho_a \overline{w^2} \tag{4}'$$

in which ζ denotes a water surface elevation from the still water level, $z = 0$. Taking into consideration that $dP/dx = 0$ and $dP/dy = 0$ at $z = \infty$, the water surface elevation can be obtained easily. Assuming that a profile of discharged buoyant water is rectangular in order to simplify the equation, ζ is given as a function of the discharged water depth H by :

$$\zeta(x,y) = (\rho_a - \rho) H/\rho \tag{5}$$

Using Eq. 5, Eq. 4' becomes :

$$P + \rho_a \overline{w^2} = \int_{\zeta}^{z} \rho g \, dz = \rho g (z + \zeta) = \{\rho_a z + \Delta\rho (H - z)\} g \tag{6}$$

Substitution of Eq. 6 into Eq. 3 and integration of Eqs. 1, 2 and 3 over the entire y-z plane of discharged buoyant water yield the following equations.

$$\frac{d}{dx}(UBH) = (E_h H + E_v B) U \tag{7}$$

$$\frac{d}{dx}(\Delta\rho g UBH) = 0 \tag{8}$$

$$\frac{d}{dx}(2U^2 BH) = -\frac{d}{dx}\left(\frac{\Delta\rho}{\rho_a} g BH\right) \tag{9}$$

where, H, B = depth and half width of discharged buoyant water, and E_h, E_v = lateral and vertical entrainment coefficients. The entrainment velocity can be formulated as the product of its coefficient and a characteristic velocity, such

as $E_h U$ and $E_v U$ in the lateral and vertical directions, respectively. Moreover, $\partial w^2 / \partial x$ is eliminated because of a neglegible small term.

Transform of the above equations into a more convenient form yields the following equations:

$$\frac{d\Delta\rho}{dx} = -\Delta\rho\left(\frac{E_h}{B} + \frac{E_v}{H}\right) \tag{10}$$

$$\frac{dH}{dx} = \frac{H}{Fd^2 - 1}\left\{(1 - 2Fd^2)\frac{1}{2B}\frac{dB}{dx} + (2Fd^2 - \frac{1}{2})\left(\frac{E_h}{B} - \frac{E_v}{H}\right)\right\} \tag{11}$$

$$\frac{dU}{dx} = \frac{U}{Fd^2 - 1}\left\{\frac{1}{2B}\frac{dB}{dx} - (Fd^2 + \frac{1}{2})\left(\frac{E_h}{B} + \frac{E_v}{H}\right)\right\} \tag{12}$$

in which, $Fd = U/\sqrt{(\Delta\rho/\rho_a)gH}$ = the densimetric Froude number.

In order to complete these equations, it is necessary to determine the lateral and vertical entrainment coefficients, E_h and E_v, and the lateral spreading rate, dB/dx, in advance. All of these factors are directly influenced by the buoyancy effects. We cannot help introducing the characters peculiar to the density flows into these additional conditions, that is a characteristic of the integral formulation as well as its fault. Although some investigators(4)(5) have tried to analyze the momentum equation in the lateral direction or the energy equation of mean flow including above equations simultaneously, these analytical methods have defects to require another assumptions awaiting solution.

In this formulation, E_h and dB/dx are given as a function of the densimetric Froude number Fd based on experimental knowledges(2). The lateral spread dB/dx is, of course, caused by the pressure difference due to the density profile within a buoyant surface discharge, which must be considered dynamically in constructing a model. In this formulation, however, its effect is limited to be taken into account statically in terms of the water surface elevation.

In the presence of vertical density gradient, as the vertical movements of fluid are restricted, the turbulent intensities and the turbulent transfer rates are diminished. These phenomena can be explained in terms of the overall Richardson number $Ri = 1/Fd^2$, which represents a degree of stratification. The relationship between E_v and Ri can be formulated based on experimental results of Ellison and Turner(6) and the authors(7) as follows :

$$E_v = \frac{0.0219\,(\,2.23 - Ri\,)}{(\,Ri^2 - 1.17Ri + 8.62\,)\,Ri^{0.9}} \tag{13}$$

On the other hand, the relationship between dB/dx and Ri has not yet been authorized. The rate of increase in the width B is generally assumed as a simple sum of the contribution due to lateral mixing and entrainment of a homogeneous (or non-buoyant) jet and the contribution due to lateral gravitational spread as follows,

$$\frac{dB}{dx} = \left(\frac{dB}{dx}\right)_{nb} + \left(\frac{dB}{dx}\right)_b \tag{14}$$

The subscripts, nb and b, denote the non-buoyant term and the buoyant one, respectively.

It is confirmed by the authors' experiment(2) that the lateral spreading rate due to buoyancy alone can be expressed by means of the spreading velocity of density-induced front motion. The term $(dB/dx)_b$ is given as follows:

$$\left(\frac{dB}{dx}\right)_b = \frac{1}{\sqrt{Fd^2 - 1}} \tag{15}$$

which is a similar form of Prych's formulation(9). Moreover, the value of $(dB/dx)_{nb}$ is adopted 0.115 as published by Tollmien(10), because the lateral mixing would be constant regardless of the density difference. E_h is also adopted the value of a homogeneous jet, $E_o = 0.075$.

CHARACTERISTICS OF INTEGRATED EQUATIONS AND FLOW REGIMES

Classification of flow regimes

It is well known that, in an estuary with well-developed salinity wedge, a river effluent flows with a transition from a densimetrically sub-critical flow ($Fd \leq 1.0$) to a supercritical one ($Fd > 1.0$), and subsequently it spreads on all sides above the sea water with depth decreasing because the buoyancy due to the density difference between fresh and salt waters plays predominant roles. It is obvious from this fact that a control section always appears near a river mouth, in which the densimetric Froude number Fd becomes a critical value 1.0. In such a case, the denominators of Eqs. 11 and 12 take the value 0.0 at the control section. Consequently, the depth and the velocity variations of river effluent, dH/dx and dU/dx become infinite. Since this tendency is certainly inconsistent with real phenomena, both numerators and denominators in Eqs. 11 and 12 must become 0.0 at the same time in order to avoid this contradiction.

Suppose that the buoyancy plays a predominant part in the lateral spread of buoyant surface discharges and that the lateral mixing does not contribute to the spread, the above-mentioned condition yields the following formula :

$$S_d = \frac{E_v(2B/H)}{dB/dx} = \frac{2}{3} \tag{16}$$

For a river effluent, Eq. 16 must be always satisfied near a river mouth. This newly-defined parameter Sd has a significant meaning that a lateral spreading rate dB/dx is expressed as a function of not only a vertical entrainment rate E_v but also an aspect ratio 2B/H of discharged buoyant water. Eq. 16 is similar to the relation, $E_v/kH = 1/2$, which has been proposed by Kashiwamura(11) providing that the streamline of river effluents increases exponentially with distance downstream from a river mouth ($dB/dx = kB$). A difference of both expressions arises from the discrepancy of pressure term in Eq. 9.

Field observations have made clear that river effluents spread above the sea water with decreasing of the water depth, while thermal discharges spread with increasing of the water depth because of an intense entrainment of ambient water. Furthermore, it was pointed out by Kashiwamura and Yoshida(12) that a flow acceleration appears near a river mouth and it is a characteristic of river effluent expansion. The conditions for classification of these phenomena are easily obtained by examining the plus and minus sign of Eqs. 11 and 12. Besides, the streamwise variation of the densimetric Froude number Fd is calculated by means of Eqs. 10, 11 and 12.

$$\frac{dFd}{dx} = \frac{Fd(Fd^2 + 1)}{2(Fd^2 - 1)}\left\{\frac{1}{2B}\frac{dB}{dx} - \frac{3}{2}\frac{E_h}{H}\right\} \tag{17}$$

It is proved from Eq. 17 that Fd tends to decrease in the streamwise direction under the condition of $Sd > 2/3$, while Fd increasing in the opposite case.

The relationships of Eqs. 11, 12 and 17 can be illustrated as a function of Sd and Fd. When considered on the basis of Fig. 2, the behavior of buoyant surface discharges can be classified into four flow regimes as follows :

Regime I	:	$dH/dx > 0$,	$dU/dx < 0$,	$dFd/dx < 0$.
Regime II	:	$dH/dx < 0$,	$dU/dx < 0$,	$dFd/dx < 0$.
Regime III	:	$dH/dx < 0$,	$dU/dx < 0$,	$dFd/dx > 0$.
Regime IV	:	$dH/dx > 0$,	$dU/dx > 0$,	$dFd/dx > 0$.

Regime I is a densimetrically super-critical flow with increasing the water depth which is usually observed in a jet-like flow, and regime II is the same with decreasing both the water depth and the velocity. On the other hand, regime III and IV are densimetrically sub-critical. In particular, regime IV is a flow acceleration, in which the velocity increases with downstream distance.

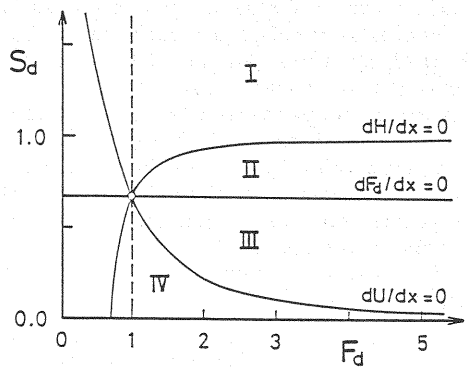

Fig. 2 Characteristics of integrated basic equations and classification of flow regimes

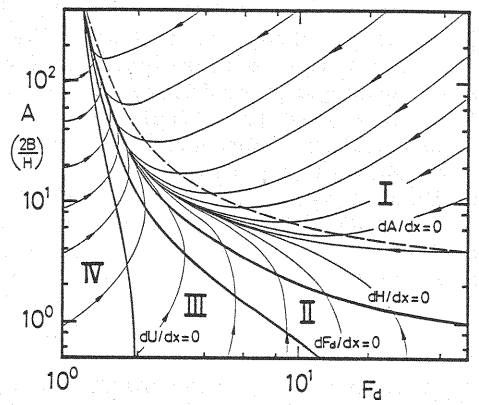

Fig. 3 Classification and numerical results as a function of A (= 2B/H) and Fd

Effects of aspect ratio

Assume that Eqs. 13, 14 and 15 are given for describing the vertical entrainment and the lateral spread of buoyant surface discharges, it is possible to explain the classification of flow regimes from I to IV in terms of an aspect ratio, A (= 2B/H) and the densimetric Froude number, Fd. These classifications as well as numerical results are illustrated in Fig. 3. The fine lines in the figure denote the numerical results, in which E_h and $(dB/dx)_{nb}$ are 0.075 and 0.2 respectively, and the arrows indicate the movements of discharged buoyant water.

A numerical simulation makes clear that buoyant surface discharges flow tending to meet one of the theoretical curves such as dH/dx = 0 at last. Based on Figs. 2 and 3, the near field behavior of buoyant surface discharges will be explained as follows.

In the case that the discharged densimetric Froude number is about 1.0, the water body flows accelerating to begin with regardless of the value of its aspect ratio. It belongs to regime IV. It is estimated that a usual river effluent always spreads with an acceleration near a river mouth, although its acceleration range may be a function of its aspect ratio. In the case that an aspect ratio is comparatively small and that the densimetric Froude number is a little larger, the velocity and the depth of effluent decrease at first (regime III) near the river mouth. A monotonous increase in Fd at regime III produces so intense entrainment that the effluent soon changes to regime II, in which Fd tends to decrease and the water depth increases to approach the final depth that satisfies the relation of dH/dx = 0.0. It is verified from this fact that a river effluent flows with a transition of flow regime from IV to III, and to II. This tendency agrees with experimental data published by the authors(2). This transition is so much sensitively influenced by the variations of dH/dx and dU/dx that there is a possibility of maintaining the relationship that dFd/dx > 0.0. Judging from the numerical simulation, however, the movement of dFd/dx is considerably unstable : so that the solution would tend to diverge in no time for the case when the relationship between E_v and Fd is not given skillfully in simulating.

On the other hand, in the majority cases of thermal discharges from energy plants, their densimetric Froude numbers at the outfall are a range of 5 - 20. Although there appears a flow of regime II or III depending on a smaller aspect ratio, in most cases, the momentum flux of discharged buoyant water forms itself into a prevailing jet flow from the outfall. Hence, it flows with depth increasing to begin with (regime I). Since there are a rapid decrease in the initial momentum and a gradual decrease in the entrainment with decreasing Fd, the discharged buoyant water gradually makes a change to a stratified-like flow (regime II). However, the transition of flow regime from I to II is rare in Fig. 3. It is due to the assumption that the profiles of velocity and density difference of discharged water are also rectangular. In buoyant surface jets,

their profiles change with downstream distance from a Gaussian one to a uniform one. And so, the vertical entrained volume becomes smaller as compared with the case of rectangular profiles, which is evaluated by means of Eq. 13. The regime II tends to appear at a final stage in such buoyant surface jets.

Although the above-mentioned discussions with respect to Fig. 3 are based on the assumptions of Eqs. 13, 14 and 15, it is worthy of understanding the variations of velocity, water depth and the densimetric Froude number accompanied with movements of buoyant surface discharges. Besides, it should be emphasized that the aspect ratio at the outfall, which has not been considered so much, becomes one of essential factors to determine the flow regime.

NUMERICAL EXAMPLES

Effluent expansion of river water

Figures 4 - 6 show numerical results in the case that the initial densimetric Froude number Fd_0 is equal to 1.2. The simulation was executed under the condition that only a half width B_0 at an outfall was changeable while a velocity U_0 and a depth H_0 were fixed. The basic equations are Eqs. 10 - 15. A abscissa in these figures denotes the distance from an outfall represented in a conventional form devided by $2B_0$.

Figure 4 shows the streamwise variations of dimensionless velocity, U/U_0 and density difference, $\Delta\rho/\Delta\rho_0$. In all cases of $2B_0/H_0$ = 0.5 - 4.0, it flows accelerating over the range of x/B_0 < 2.0, where the value of velocity equals about $1.15U_0$. After that, the velocity tends to decrease in all cases. The rate of decreasing in both velocity and density difference becomes the -1/2 power of x/B_0, which coincides with the rate of a plane homogeneous turbulent jet.

Figures 5 and 6 also show the streamwise variations of half width B, water depth H and the densimetric Froude number Fd. The smaller the aspect ratio is, in which an intense acceleration is observed, the sooner the depth decreases and the width

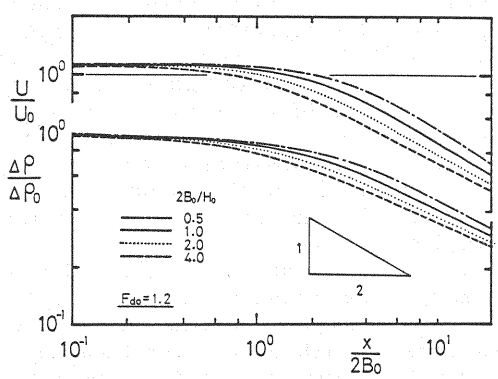

Fig. 4 Decay of velocity and density difference along streamwise axis in case of Fd_0 = 1.2

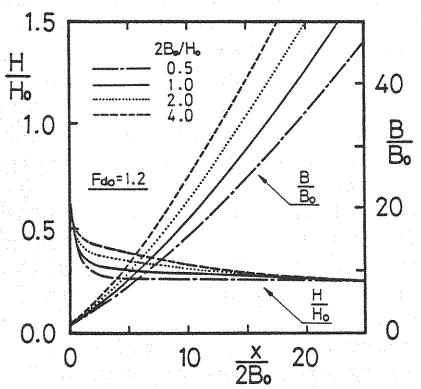

Fig. 5 Variation of half width and water depth in case of Fd_0 = 1.2

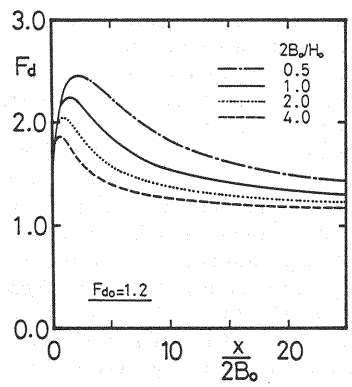

Fig. 6 Variation of densimetric Froude number in case of Fd_0 = 1.2

does not spread near the river mouth. It indicates that the aspect ratio of discharged water body in addition to a decrease in water depth may have a strong influence on the flow acceleration phenomenon. If the spreading rate of the half width is expressed in terms of $dB/dx = kB$, the value of k equals 10^{-5} (1/cm) approximately, which is in good agreement with the field data(12) observed at Ishikari river at Hokkaido, Japan.

As shown in Fig. 6, the position in which Fd becomes a maximum value, is located downstream of the flow acceleration region. According to these results, it is conjectured that a river effluent discharged with Fd = 1.0 flows with a transition from regime IV to III, and II in which $dFd/dx < 0.0$.

Spread of thermal discharge

In a buoyant surface jet with larger densimetric Froude numbers, it is already confirmed that the lateral and vertical profiles of velocity and density difference are geometrically similar and approximated by a Gaussian curve. Their functional expressions are as follows :

$$U(x,y,z) = U_s(x)\, f_1(y/B_e)\, f_1(z/H_e) \qquad (18)$$
$$\Delta\rho(x,y,z) = \Delta\rho_s(x) f_2(y/B_e)\, f_2(z/H_e)$$

in which

$$f_1(t) = \exp(-t^2) \quad ; \quad f_2(t) = \exp(-t^2/2) \qquad (19)$$

For these equations, $U_s(x)$, $\Delta\rho_s(x)$ = surface velocity and surface density difference on the jet axis, and B_e, H_e = width and depth at a fixed point where U/U_s is 1.0/e (= 0.3679).

In much the same way as a rectangular profile of river effluent, substitution of Eq. 18 into Eq. 3 and integration of the basic conservation equations over the range of $z = -\zeta - \infty$ and $y = -\infty - \infty$, moreover transform of integrated equations yields the following equations :

$$\frac{d\Delta\rho_s}{dx} = -\Delta\rho_s\left(\frac{2E_h}{I_1 B_e} + \frac{E_v}{I_2 H_e}\right) \qquad (20)$$

$$\frac{dH_e}{dx} = \frac{H_e}{(I_3 I_4 Fd_s^2 - 2I_7)}\left\{(2I_3 I_4 Fd_s^2 - I_7)\left(\frac{2E_h}{I_1 B_e} + \frac{E_v}{I_2 H_e}\right) - (I_3 I_4 Fd_s^2 - I_7)\frac{1}{B_e}\frac{dB_e}{dx}\right\} \qquad (21)$$

$$\frac{dU_s}{dx} = \frac{U_s}{(I_3 I_4 Fd_s^2 - 2I_7)}\left\{I_7\frac{1}{B_e}\frac{dB_e}{dx} - (I_3 I_4 Fd_s^2 - I_7)\left(\frac{2E_h}{I_1 B_e} + \frac{E_v}{I_2 H_e}\right)\right\} \qquad (22)$$

where

$$I_1 = \int_{-\infty}^{\infty} f_1(t)dt \quad ; \quad I_2 = I_1/2 \quad ; \quad I_3 = \int_{-\infty}^{\infty} f_2(t)dt \quad ;$$
$$I_4 = I_3/2 \quad ; \quad I_7 = 2.4533 \quad ; \quad Fd_s = U_s/\sqrt{(\Delta\rho_s/\rho_a)gH}$$

In a derivation of the above equations, a sectionally integrated coefficient I_7 is calculated through expanding the pressure term dP/dx in a Maclaurin series, since it is impossible to integrate its term immediately with respect to z because of including the water surface elevation.

The numerical simulation can be performed based on Eqs. 20, 21, 22, 13 and 14. It is, of course, necessary to rewrite the last two equations in a form considering the profiles of U and $\Delta\rho$. Since the self-preserving of their profiles holds good only at the region of established flow, initial conditions must be given at the initial point of that region. A treatment of this region cannot but

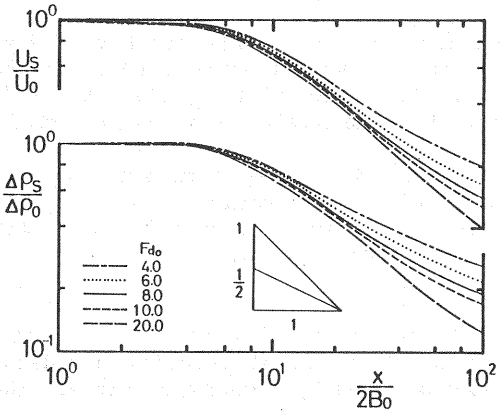

Fig. 7 Decay of velocity and density difference along streamwise axis as a function of Fd_o

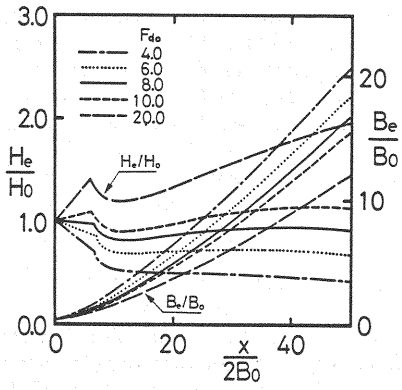

Fig. 8 Variation of half width and water depth as a function of Fd_o

rely upon experimental results. In this numerical simulation, experimental formulae proposed by Stefan et al.(13) are in use, whose experiment is only minute measurements at the zone of flow establishment.

Figures 7 - 9 show numerical results of Fd_o = 4 - 20 in the same manner as Figs. 4 - 6. The rate of decreasing in velocity becomes smaller as the initial densimetric Froude number is smaller or as it flows with downstream distance from the outfall. In the case of Fd_o = 20, its rate obeys the -1 power of x/B_o, which has been observed at a three-dimensional homogeneous jet. On the other hand, in the case of Fd_o = 4, it approaches the -1/2 power of a plane homogeneous jet. And more, the rates of Fd_o = 6, 8 and 10 are caught in both rates. It is proved from these facts that as the gravitational stability due to buoyancy promotes, the behavior of discharged buoyant water changes from a three-dimensional to a plane jet. The rate of decreasing in density difference $\Delta\rho/\Delta\rho_o$ is smaller compared with one in velocity U/U_o.

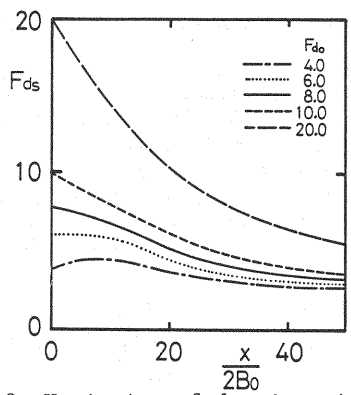

Fig. 9 Variation of densimetric Froude number as a function of Fd_o

As Fig. 8 shows, the numerical simulation predicts well the whole features of buoyant surface jet that the vertical spread is counteracted because of the stratification, while the lateral spread is promoted. At the same time, the value of Fd_s decreases monotonously downstream to approach a constant value. Based on the results of Figs. 7, 8 and 9, it may be concluded that buoyant surface discharges with larger densimetric Froude numbers bahave like a jet-like flow (regime I) near the outfall, and get on to a flow of regime II with increasing the buoyancy effects.

Discontinuous points in those figures indicate the end of the flow establishment region. The numerical simulation is started downstream from these points using initial conditions given beforehand.

CONCLUSIONS

Through an integral formulation, the near field behavior of buoyant surface discharges became clear as the following conclusions :

(1) Taking the characteristics of integrated basic equations into consideration, buoyant surface discharges are classified into four flow regimes, as shown schematically in Figs. 2 and 3. Its classification is a function of two parameters, Fd and Sd (= $E_V(2B/H)/(dB/dx)$). The latter suggests that the lateral spread is closely correlated with not only the vertical entrainment rate but also its aspect ratio.

(2) In the case of river effluents with smaller densimetric Froude numbers, the aspect ratio is an essential factor in determining the near field bahavior.

(3) The presence of a flow acceleration observed in river effluent expansion is verified theoretically through this classification, and it was confirmed by a numerical simulation assuming that a profile of discharged buoyant water is rectangular.

(4) When the lateral spread due to buoyancy alone can be explained in terms of the density-induced front motion, a numerical simulation can fairly well predict the whole features of river effluents as well as thermal discharges.

REFERENCES

1. Murota, A., K. Nakatsuji and Y. Shibagaki : Field survey of effluent expansion from river mouth, Proc. 31st Japanese Conf. on Coastal Eng., pp.630-634, 1984b (in Japanese).
2. Murota, A., K. Muraoka and K. Nakatsuji : Initial entrainment and lateral spread of three-dimensional buoyant surface jet, J. Hydroscience and Hydr. Eng., Vol.1, No.2, pp.33-51, 1983.
3. Murota, A., K. Nakatsuji and Y. Shibagaki : Buoyancy effects on near field behavior of three-dimensional buoyant surface discharges, Proc. 28th Japanese Conf. on Hydraulics, pp.113-120, 1984a (in Japanese).
4. Hayashi, T. and M. Arita : Study on mathematical model on the spread of heated water, Proc. 20th Japanese Conf. on Hydraulics, pp.161-172, 1976 (in Japanese).
5. Komatsu, T. and T. Tsubaki : On the three dimensional stratified surface jet, Proc. 22nd Japanese Conf. on Hydraulics, pp.1-6, 1978 (in Japanese).
6. Ellison, T.H. and J.S. Turner : Turbulent entrainment in stratified flow, J. Fluid Mech., Vol.4, pp.423-448, 1959.
7. Murota, A. and K. Nakatsuji : Turbulent entrainment in plane buoyant surface jet, Proc. JSCE, Vol.351/II-1, pp.96-107, 1984a (in Japanese).
8. Koh, R.C.Y. : Two-dimensional surface warm jets, Proc. ASCE, Vol.97, HY6, pp. 819-836, 1971.
9. Prych, E. : An analysis of a jet into a turbulent fluid, Water Research, Vol. 17, pp.647-657, 1973.
10. Tollmien, W. : Berechnung Turbulenter Ausbreitungsvorgange, ZAMM, Vol.6, pp. 468-478, 1926.
11. Kashiwamura, M. : Mechanism of river effluents, Proc. 17th Japanese Conf. on Hydraulics, pp.56-60, 1973 (in Japanese).
12. Kashiwamura, M. and S. Yoshida : Phenomenon of river effluents, Proc. 17th Japanese Conf. on Coastal Eng., pp.219-223, 1970 (in Japanese).
13. Stefan, H., J. Bergstedt and E. Mrosla : Flow establishment and initial entrainment of heated water surface jets, St. Anthony Falls Hydr. Labo., Univ. of Minnesota, EPA-660/3-75-014, 1975.

APPENDIX - NOTATION

The following symbols are used in this paper :

A	= aspect ratio (= 2B/H);
B, B_e	= width of water discharged;
E_h, E_V, E_o	= entrainment constant;
Fd, Fd_s	= densimetric Froude number;
$f_1(t)$, $f_2(t)$	= similarity function regarding $U(y,z)$ and $\Delta\rho(y,z)$;
g	= gravitational acceleration;

H, H_e	= depth of water discharged;
I_1, I_2, .. I_7	= sectionally integrated coefficients;
k	= constant ($dB/dx = kB$);
P	= pressure;
Ri	= overall Richardson number;
Sd	= $E_V(2B/H)/(dB/dx)$;
U, V, W	= velocity component in x, y and z directions;
u, v, w	= fluctuating part of velocity;
$-\overline{uv}$, $-\overline{uw}$	= turbulent momentum flux;
x, y, z	= coordinate (sketched in Fig. 1);
ζ	= water surface elevation;
ρ	= density;
ρ_a	= density of ambient water;
$\Delta\rho$	= density difference (= $\rho - \rho_a$); and
$-\overline{\rho v}$, $-\overline{\rho w}$	= turbulent density flux.

Subscripts :

b	= buoyant discharge;
e	= depth or width defined as $U = U_s/2.718$;
h	= lateral direction;
nb	= non-buoyant discharge;
o	= outlet;
s	= water surface; and
v	= vertical direction.